INTERNATIONAL JOURNAL FOR NUMERICAL METHODS IN FLUIDS, VOL. 9, 263–273 (1989)

NUMERICAL SIMULATION OF THE HYDRODYNAMIC INTERACTION BETWEEN A SEDIMENTING PARTICLE AND A NEUTRALLY BUOYANT PARTICLE

MARC S. INGBER

Department of Mechanical Engineering, University of New Mexico, Albuquerque, New Mexico 87123, U.S.A.

SUMMARY

A new method for the simulation of the translational and rotational motions of a system containing a sedimenting particle interacting with a neutrally buoyant particle has been developed. The method is based on coupling the quasi-static Stokes equations for the fluid with the rigid body equations of motion for the particles. The Stokes equations are solved at each time step with the boundary element method. The stresses are then integrated over the surface of each particle to determine the resultant forces and moments. These forces and moments are inserted into the rigid body equations of motion to determine the translational and rotational motions of the particles. Unlike many other simulation techniques, no restrictions are placed on the shape of the particles. Superparametric boundary elements are employed to achieve accurate geometric representations of the particles. The simulation method is able to predict the local fluid velocity, resolve the forces and moments exerted on the particles, and track the particle trajectories and orientations.

KEY WORDS Low-Reynolds-number flow Sedimentation Hydrodynamic interactions Two-phase flows Suspensions Boundary element method

INTRODUCTION

Particles suspended in fluids play an important role in many scientific and engineering problems, including pipeline transport of slurries, petroleum recovery, composite materials processing and blood flow. The prediction of the rheological properties of suspensions is thus an important concern. One particular method of determining the relative viscosities of suspensions is with the use of a falling ball rheometer.[1, 2] Falling ball rheometry is based upon Stokes' law for a sphere sedimenting in a large expanse of fluid at rest. The hydrodynamic interaction with the suspensions causes additional drag and the Stokes' law must be modified. In the case of a dilute suspension, it is sometimes possible to predict the behaviour of the suspension by considering the hydrodynamic interaction between just two of the particles. Numerical work in this field has been limited because of the complexities of modelling these microstructure–flow interactions. This paper presents a boundary element method with which to study the hydrodynamic interactions between a sedimenting particle and a neutrally buoyant particle.

Several methods have been developed in the past to calculate hydrodynamic interactions between immersed particles. Happel and Brenner[3] used the method of reflections to study the two-sphere problem. Further studies of the two-sphere problem were conducted by O'Neill and Majumdar[4] using bispherical co-ordinates and by Ganatos *et al.*[5] and Kim and Mifflin[6] using a boundary collocation method based on an expansion of Stokes equations into appropriate eigenfunctions. Kim[7] extended the method of reflections to the case of prolate spheroids. Durlofsky *et al.*,[8] by using the resistance matrix, were able to simulate the multibody problem.

0271–2091/89/030263–11$05.50

Received 4 January 1988
Revised 17 May 1988

However, all of these methods are limited to systems of high symmetry to reduce the number of unknowns.

Although other numerical methods such as the finite difference (FD) and finite element (FE) methods are not limited to symmetric shapes, they pose difficult problems in performing the discretization. For the exterior problem, disturbances caused by the particles decay very slowly and thus a very large computational domain is necessary. Even for the interior problem, at each time step a new grid is required because of particle translation and rotation. The boundary element method (BEM) is well suited to this class of problems. As with FD and FE methods, the BEM is not restricted by the geometry. Since the BEM requires only the discretization of the boundary, the discretization can be translated and rotated with the particles. In particular, there is no distortion of the elements when the particles are rigid.

The present study is based on a quasi-steady analysis of multiparticle Stokes flow interactions. Neglecting virtual mass and particle acceleration,[9] the Stokes equations are solved at each time step using the BEM. The resultant force and moment on each particle is determined by integrating the stress field over the surface of each particle. These forces and moments are then used in the rigid body equations of motion to translate and rotate the particles. The efficiency of the BEM in determining the quasi-steady solutions makes it possible to follow the trajectories of sedimenting particles over many diameters.

PROBLEM FORMULATION

Consider the creeping flow in domain Ω past two particles P_1 and P_2 of arbitrary shape, where surfaces Γ_1 and Γ_2 respectively appear as shown in Figure 1. The governing differential equations in terms of the dimensionless perturbed fluid velocity u_i and pressure p are given by

$$\frac{\partial^2 u_i(x)}{\partial x_j \partial x_j} = \frac{\partial p(x)}{\partial x_i}, \qquad \frac{\partial u_i(x)}{\partial x_i} = 0, \qquad x \in \Omega, \tag{1}$$

where Cartesian tensor notation is employed. The perturbed fluid velocity satisfies the non-slip boundary condition on the solid surface; that is,

$$u_i(x) = -U_i(x), \qquad x \in \Gamma, \tag{2}$$

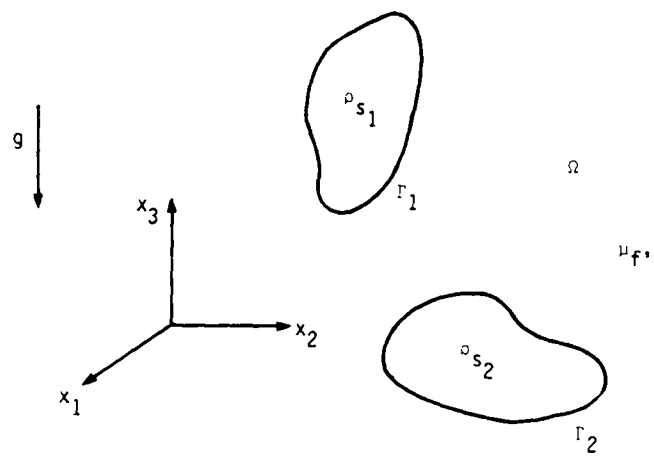

Figure 1. Problem geometry

where Γ is the union of Γ_1 and Γ_2. At infinity, the velocity and pressure must possess the following asymptotic behaviour:

$$u_i(x)=O(R^{-1}) \quad \text{and} \quad p(x)=O(R^{-2}) \quad \text{as } R\to\infty, \tag{3}$$

where R is the distance from the origin to a point in the flow field.

The fundamental solution for this set of differential equations is given by[10, 11]

$$u_{ij}^*(x, y)=\frac{1}{8\pi r}(\delta_{ij}+r_{,i}r_{,j}), \tag{4}$$

$$p_j^*(x, y)=\frac{r_{,j}}{4\pi r^2}, \tag{5}$$

where $r=|x-y|$ and the comma denotes partial differentiation with respect to the appropriate Cartesian co-ordinate. Physically, u_{ij}^* represents the ith component of velocity at the point x due to a point force in the j-direction at the point y; p_j^* is the corresponding pressure. By considering a weighted residual statement of the differential equations with weighting functions given by the fundamental solutions (see e.g. Brebbia *et al.*[12]), one may represent u_i by a boundary integral as follows:

$$c_{ij}(\xi)u_j(\xi)+\int_\Gamma q_{kji}^*(\xi, x)u_k(x)n_j(x)\mathrm{d}\Gamma=-\int_\Gamma u_{ik}^*(\xi, x)f_k(x)\mathrm{d}\Gamma, \tag{6}$$

where

$$q_{ijk}^*=\frac{-3}{4\pi}\frac{r_{,i}r_{,j}r_{,k}}{r^2}, \tag{7}$$

the f_ks are the components of stress along the surface Γ, and the n_js are the components of the unit outward-normal vector to the boundary Γ. The coefficient tensor c_{ij} appears, since in applying the divergence theorem to obtain the boundary integral equation (BIE, equation (6)), a portion of the domain about the field point ξ must be excluded in order to avoid the isolated singularity. Although the entries in the tensor can be determined from the geometry of the domain, it is simpler to evaluate them numerically by considering the case of uniform flow, from which it follows:

$$c_{ij}(\xi)=\int_\Gamma q_{kji}^*(\xi, x)n_k(x)\mathrm{d}\Gamma. \tag{8}$$

Assuming that the velocities are known at a given time t, the BIE (equation (6)) represents a Fredholm equation of the first kind for the unknown stresses. In order to solve the BIE numerically, the boundary is discretized into N boundary elements and within each element the unknown stresses are assumed to be constant. (Reasons for the selection of the constant strength element are discussed below.) By applying the BIE (equation (6)) at the centroid of each element, one can generate a system of $3N$ linear equations in the $3N$ unknown components of stress. These stresses can then be integrated over the surface of the particles to determine the resultant force and moment.

Although a complete description of the motion of the particles should contain the unsteady forces, their inclusion into the analysis would require prohibitive computational costs. Leichtberg *et al.*[9] showed that except for start-up flows, the unsteady forces were of negligible importance. In the present study a quasi-static analysis is performed. That is, after an initial velocity (linear and angular) for the particles is assumed, the steady Stokes equations are solved by use of the

boundary element equations. At each time step the velocity, angular velocity, position and orientation of the particles are updated with the rigid body equations of motion.

Several different types of boundary elements were tested in order to optimize the computer code. Previous studies[13, 14] showed that relatively small changes in geometry can result in substantial changes to the flow field in the creeping flow regime. In order to approximate the geometry accurately, a superparametric boundary element was selected. In fact, when flat boundary elements were tested, the stress field oscillated about the true value. The oscillations disappeared when the boundary was approximated with the superparametric elements. Constant, linear and quadratic approximations for the source strengths were also tested. Although successively higher orders of approximation in the source strengths provided more accurate results, the number of unknowns also increased. Because some simulations could require up to 4500 time steps, constant strength elements were chosen because they required the least computational effort.

Several different time integration procedures were also tested: a fourth-order Runge–Kutta scheme; a variable time step, fifth-order Runge–Kutta scheme; a variable order Adams–Bashford–Moulton scheme; and a scheme using the Euler explicit method in the linear and angular velocities and third-order differencing in the displacements and rotations. Although the variable step Runge–Kutta and variable order Adams–Bashford–Moulton schemes were efficient in the sense that they automatically adjusted the time step to be as large as possible within stability limitations while at the same time keeping the local error within prescribed bounds, they proved to require the most computer time. The vast majority of the computational effort was spent in evaluating the derivatives, that is, the forces and moments required in the rigid body equations of motion. Therefore schemes with elaborate error analysis were very expensive. In fact, the simple differencing scheme described below proved to be the most practical in terms of speed and accuracy.

In order to simplify the kinematics, only problems in which the centres of the two particles are contained in a vertical plane of symmetry are considered. With this simplification, the translation of the particles is confined to the plane of symmetry and the rotation of the particles is confined to the axis perpendicular to the plane of symmetry. In these cases the rigid body equations of motion can be reduced to six first-order equations for each particle. (It should be noted that this simplification is not required by the BEM as the BEM provides fully three-dimensional results). The equations of motion are written below:

$$\begin{aligned}
\frac{dy_i}{dt} &= v_i, & \frac{dv_i}{dt} &= \frac{F_{y_i}}{\rho_{si} V_i}, \\
\frac{dz_i}{dt} &= w_i, & \frac{dw_i}{dt} &= \frac{F_{z_i} - (\rho_{si} - \rho_f) V_i g}{\rho_{si} V_i}, \\
\frac{d\theta_i}{dt} &= \omega_i, & \frac{d\omega_i}{dt} &= \frac{M_{x_i}}{I_i},
\end{aligned} \tag{9}$$

where the subscript i refers to the ith particle, g is the gravitational constant, (y_i, z_i) are the components of displacement, θ_i is the rotation, (v_i, w_i) are the components of velocity, ω_i is the angular velocity, ρ_f is the density of the fluid, V_i is the volume of the particle, I_i is the moment of inertia, (F_{y_i}, F_{z_i}) are the components of the resultant force and M_{x_i} is the resultant moment calculated by the BEM.

If t^n represents the nth time step, then the y-component of displacement and velocity can be

expanded in a Taylor series as follows:

$$y_i(t^{n+1}) = y_i(t^n) + \frac{dy_i}{dt}(t^n)\Delta t + \frac{1}{2}\frac{d^2y_i}{dt^2}(t^n)(\Delta t)^2 + O(\Delta t)^3, \tag{10}$$

$$v_i(t^{n+1}) = v_i(t^n) + \frac{dv_i}{dt}(t^n)\Delta t + \frac{1}{2}\frac{d^2v_i}{dt^2}(t^n)(\Delta t)^2 + O(\Delta t)^3, \tag{11}$$

where $\Delta t = (t^{n+1} - t^n)$. Solving for dv_i/dt in equation (11) and substituting the result into equation (10) for d^2y_i/dt^2 yields

$$y_i(t^{n+1}) = y_i(t^n) + \tfrac{1}{2}[v_i(t^n) + v_i(t^{n+1})] + O(\Delta t)^3. \tag{12}$$

Similar expressions for the z_i and θ_i can be obtained as

$$z_i(t^{n+1}) = z_i(t^n) + \tfrac{1}{2}[w_i(t^n) + w_i(t^{n+1})] + O(\Delta t)^3, \tag{13}$$

$$\theta_i(t^{n+1}) = \omega_i(t^n) + \tfrac{1}{2}[\omega_i(t^n) + \omega_i(t^{n+1})] + O(\Delta t)^3. \tag{14}$$

The linear and angular velocities at the $(n+1)$th time step are determined by use of Euler explicit differencing in conjunction with equation (9). The truncation error is monitored at each time step and the time step can be adjusted upward or downward in response to this error. Although continued research is being undertaken to optimize the time integration, the method outlined above is the one used to obtain the results in this paper. In selected test problems, these results were compared with those of some of the more sophisticated schemes mentioned above as an independent check of their accuracy.

A TEST PROBLEM

In order to test the numerical algorithm, the case of two identical spheres with identical initial conditions, but with different initial positions, is considered (Figure 2). The simulation is run until steady state. This problem is considered since the BEM results at steady state can be compared with the analytic results of Stimson and Jeffrey[15] and Goldman *et al.*[16]

The spheres were given an initial sedimentation velocity approximately 50% higher than the steady state velocity for the isolated single sphere, and no initial angular velocity. For times

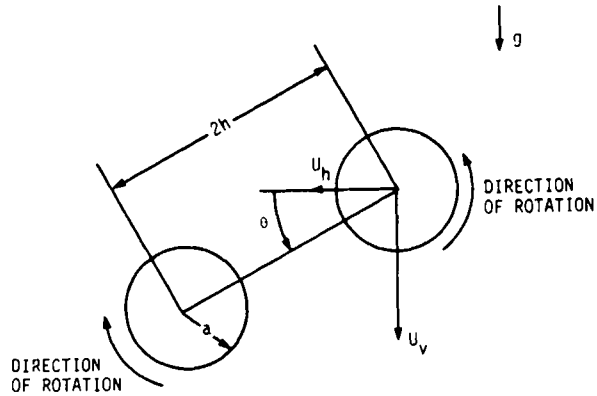

Figure 2. Two identical spheres settling at an angle

greater than zero, the particles would decelerate and spin up toward steady state conditions. It is convenient to present the results in terms of the dimensionless physical quantities. The characteristic length scale is given by the radius of the sphere a, and the characteristic velocity is given in terms of the terminal sedimentation velocity U_t of an isolated sphere:[3]

$$U_t = 2a^2(\rho_s - \rho_f)g/9\mu. \tag{15}$$

The components of the steady state velocities are given by (U_h, U_v) in the horizontal and vertical directions respectively. For cases in which $U_h = 0$, the drag correction factor λ can be defined as the ratio of terminal vertical velocity U_v to U_t since the drag is directly proportional to the velocity.

The spheres were discretized into the boundary elements by subdividing the surface into lines of longitude and lines of latitude. Hence both quadrilateral and trilateral elements were employed. Several discretizations were tested. Results are listed below for two of the discretizations. Grid A used 100 nodes to define the geometry and contained 32 boundary elements. Grid B used 244 nodes to define the geometry and contained 72 boundary elements. Generally, less than 50 time steps were necessary to obtain steady state conditions. Grid A took 1·97 CPU-s per time step while grid B took 11·67 CPU-s per time step on a CRAY XMP time-sharing system.

The results obtained by the BEM for the case of the spheres falling side by side are compared with the exact solutions in Table I. The accuracy of the BEM improved with the finer grid and also improved as the gap between the spheres was increased. There are two causes for the degradation in accuracy as the gap width was decreased. First, the boundary element program used a fixed quadrature rule, so that when field points on one sphere were close to the source points contained in a boundary element on the adjacent sphere, the singular nature of the integrand caused a growth in quadrature errors. Secondly, for closely spaced spheres there are large gradients in the stress field, making the constant strength elements less accurate. Nevertheless, errors in the drag correction factor were all less than 0·3% while the errors in the steady state angular velocity were less than 3%. Similar results for the cases of two spheres falling parallel to their lines of centres (that is, $\theta = 90°$) and for two spheres falling at various angles between their lines of centres and the horizontal are shown in Tables II and III. For the case of the two spheres falling parallel to their lines of centres, the drag correction factors compared extremely well with the exact results. Because of the flow field symmetry, the angular velocities of the spheres are zero. For the case when the angle between the lines of centres of the two objects and the horizontal is not equal to 0° or 90°, in the steady state, the particles will possess both a vertical sedimenting velocity U_v and a horizontal drift velocity U_h. Again, as seen in Table III, the BEM results compare quite well with the exact results.

An example of the transient response for the case $\theta = 45°$, $h = 1{\cdot}5431$ is shown in Figure 3. Recall that the spheres were given an initial sedimenting velocity but no initial drift or angular velocity. The sedimenting velocity U_v is seen to monotonically decrease towards its steady state value. The

Table I. Comparisons of the solutions obtained by the BEM with the exact solution for two equal spheres falling side by side

	Drag correction factor λ			Angular velocity $a\|\omega\|/U_t$		
h/a	Grid A	Grid B	Exact	Grid A	Grid B	Exact
2·000	0·8341	0·8363	0·8363	0·0476	0·0473	0·0467
1·5431	0·7918	0·7935	0·7945	0·0785	0·0782	0·0775
1·1276	0·7309	0·7323	0·7327	0·1354	0·1348	0·1314

Table II. Comparisons of the solutions obtained by the BEM with the exact solution for two equal spheres falling parallel to their lines of centres

	Drag correction factor λ		
h/a	Grid A	Grid B	Exact
2·0000	0·7405	0·7422	0·7423
1·5431	0·7004	0·7035	0·7025
1·1276	0·6575	0·6590	0·6596

Table III. Comparisons of the solutions obtained by the BEM using the fine grid (grid B) with the exact solution for two equal spheres falling at various angles θ between the line-of-centres and the horizontal at a spacing of $h = 1{\cdot}5431$

	U_v/U_t		U_h/U_t		$a\lvert\omega\rvert/U_t$	
θ	BEM	Exact	BEM	Exact	BEM	Exact
30°	1·3001	1·2998	0·0718	0·0715	0·0683	0·0671
45°	1·3423	1·3411	0·0828	0·0825	0·0560	0·0548
60°	1·3836	1·3823	0·0717	0·0715	0·0397	0·0388

drift velocity U_h and angular speed ω increase rapidly from their imposed initial conditions. The angular velocity actually slightly overshoots its steady state value before reaching steady state.

INTERACTION OF A SEDIMENTING PARTICLE WITH A NEUTRALLY BUOYANT PARTICLE

Three systems, each composed of a sedimenting particle (S) and a neutrally buoyant particle (NB), are considered (Figure 4). System 1 contains two spherical particles, whereas systems 2 and 3 contain a spherical sedimenting particle and a neutrally buoyant prolate spheroid of aspect ratio 0·5. In system 2, the major axis of the spheroid is aligned with the vertical axis, while in system 3 the major axis of the spheroid is aligned with the horizontal axis. The viscosity of the fluid is 10 Pa s. The density of the sedimenting particle is 2375 kg m^{-3}, while the density of the fluid and neutrally buoyant particle is 1182 kg m^{-3} in all cases. The radius of the sedimenting sphere is 0·2 cm, resulting in the terminal velocity of the isolated sedimenting sphere given by $U_t = 0{\cdot}02651$ cm s^{-1}. Under these conditions the Reynolds number is of the order 10^{-5}, which is well within the range of low-Reynolds-number flow.

As in the test problem, several grids were considered. However, since it was desired to run the simulation for up to 4500 time steps, grids with the same number of nodal points as in grid A of the test problem were chosen. (These results were compared those of finer discretizations run over fewer time steps as an *ad hoc* check of accuracy.) The time step ranged from a low of 0·008 s to a high of 0·025 s. The time step was periodically adjusted in response to the local truncation error.

The positions of the centres of the particles for the three systems are plotted at 2 s intervals in Figure 5. The motion of the sedimenting particle caused the neutrally buoyant particle to move vertically downward and to rotate counterclockwise. Initially, both particles bowed outward from

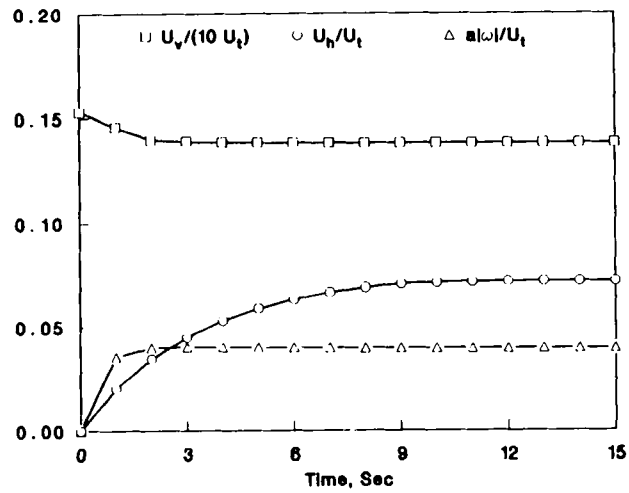

Figure 3. The transient response of two sedimenting spheres; $\theta = 45°$, $h = 1{\cdot}5431$

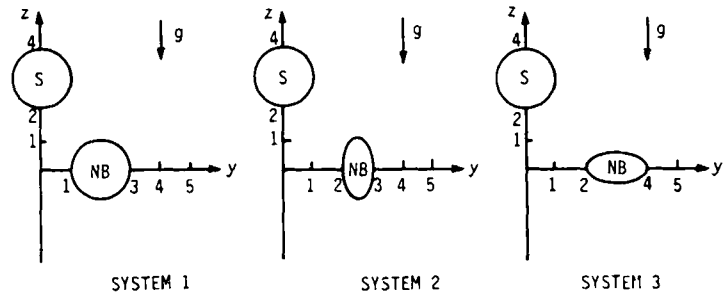

Figure 4. Three systems composed of a sedimenting particle (S) and a neutrally buoyant particle (NB)

each other. This opposing horizontal motion persisted until the sedimenting particle passed the neutrally buoyant particle, at which time the two particles moved horizontally toward each other. This behaviour was a result of symmetry of the Stokes equations. That is, because of this symmetry, a change in direction of the resultant moments and horizontal forces on the two particles was observed as the sedimenting particle moved past the neutrally buoyant particle. In fact, if the simulation was run long enough, the neutrally buoyant particle would eventually move to the left of its original horizontal position as it was dragged into the wake of the sedimenting particle. The angular velocity of the neutrally buoyant particle as a function of time is plotted in Figure 6 for the three systems. It can be seen that the maximum angular velocity occurred very close to the time at which the sedimenting particle overtook the neutrally buoyant particle, again a manifestation of the symmetry of the Stokes equations. The associated rotation of the neutrally buoyant particles ranged from 35° to 46° at the end of the simulations ($t = 36$ s).

The initial vertical positions of the centres of the two particles were chosen to be the same in all three simulations. A measure of the resistance caused by the neutrally buoyant particle on the sedimenting particle can be given by the time it takes for the centre of the sedimenting particle to reach the same vertical elevation as the neutrally buoyant particle. This time can be designated as

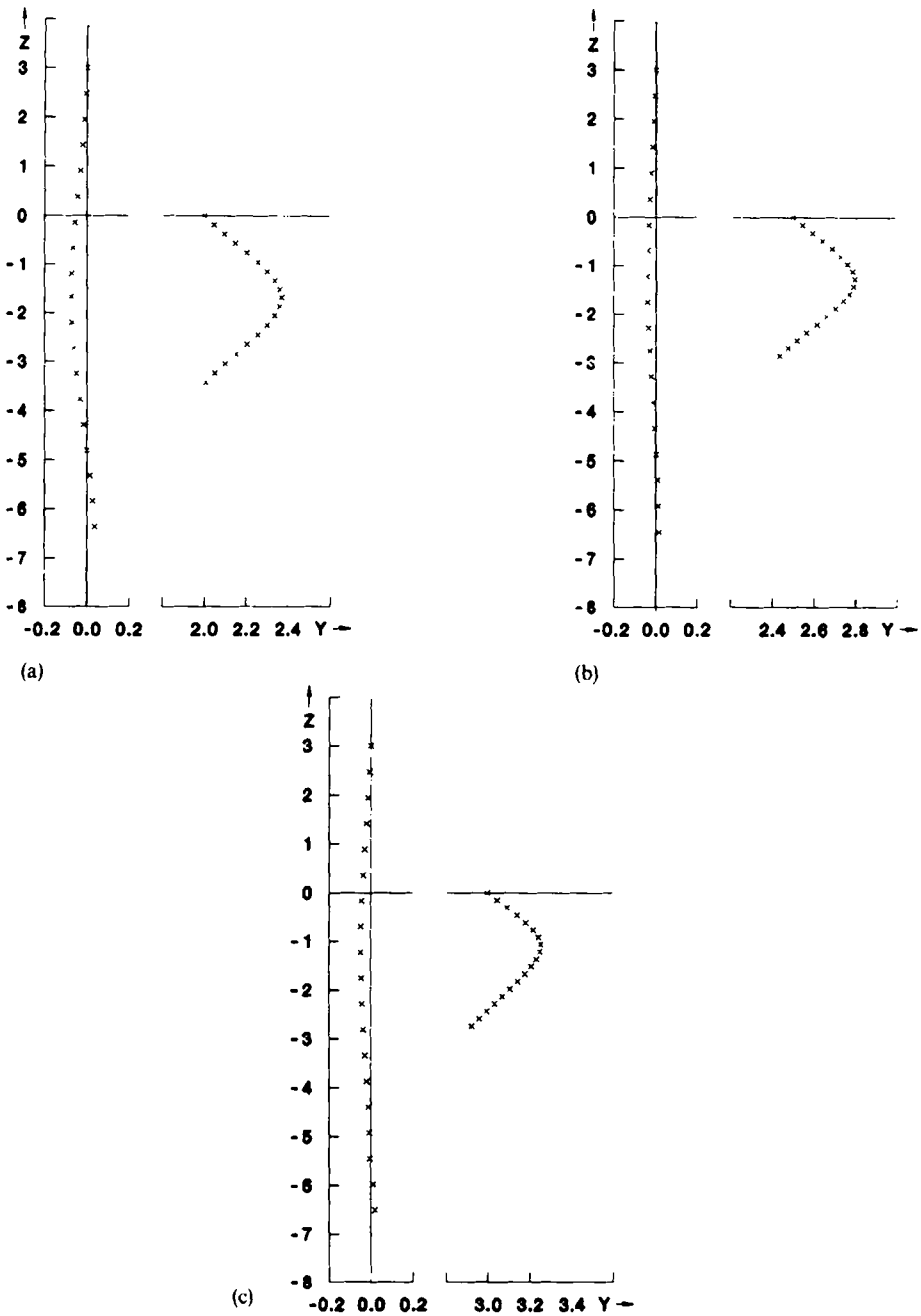

Figure 5. Trace of the locations of the centres of the two particles plotted at 2 s intervals: (a) system 1; (b) system 2; (c) system 3

the crossover time. The crossover time for system 1 was 18·2 s; for system 2, 16·2 s; and for system 3, 16·0 s. The crossover time for system 1 was larger than for the other two systems for two reasons. First, the neutrally buoyant sphere had a larger surface area than the prolate spheroids; and secondly, the particles came closer together in system 1 than in the other two systems,

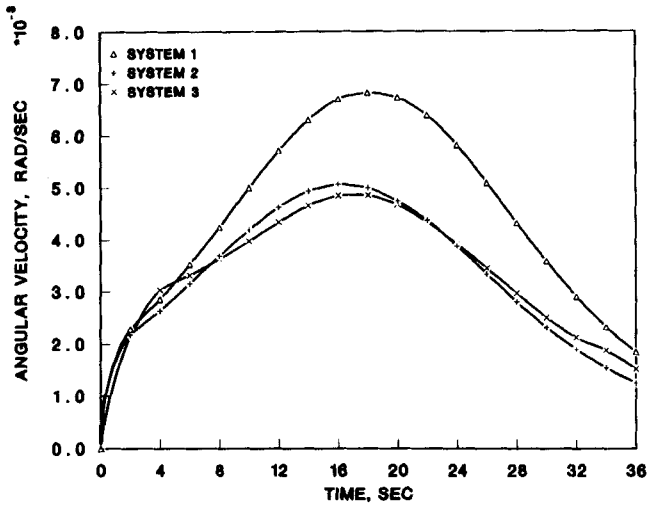

Figure 6. Angular velocity of the neutrally buoyant particle

Table IV. Maximum lateral deflections

Case	Sedimenting particle	Neutrally buoyant particle
1	−0·0734	0·369
2	−0·0498	0·296
3	−0·0471	0·252

resulting in a stronger hydrodynamic interaction. The crossover times are seen to be essentially the same for case 2 and case 3. The maximum lateral deflections of the two particles are given in Table IV. Again, since the initial horizontal position of the particles was the closest in system 1, it is to be expected that the maximum lateral deflection should be the largest in this case. The maximum lateral deflection of the prolate spheroid with major axis aligned vertically is seen to be larger than the case in which the major axis is aligned horizontally. This result is a consequence of the larger projected vertical area for the case with vertical alignment.

DISCUSSION

A numerical simulation of the hydrodynamic interaction and resultant motion of a sedimenting particle and a neutrally buoyant particle was performed by coupling a quasi-steady analysis of multiparticle Stokes flow interactions using the BEM with the rigid body equations of motion. The program was tested by allowing a system of identical particles to come to steady state and comparing the results to analytic solutions. Although this is no guarantee that the transient motion was properly simulated, it did provide some confidence in the numerical algorithm. Three systems containing a sedimenting particle and a neutrally buoyant particle were considered. The results indicated that the neutrally buoyant particle could be dragged significantly simply by the hydrodynamic interactions. The motion of the system showed some horizontal symmetry. The symmetry in the vertical direction was not evident because of the gravitational force.

Although only exterior flows containing two particles have been considered in this work, the methodology is quite general. The extension to more than two particles is simple from a programming point of view. In fact, the current BEM code is dimensioned to accept up to six particles. Further, the extension to the cases of interior flows, shear flows, extensional flows and the like requires relatively few programming changes. The major constraint at present is the computational cost. Even though the CPU time per iteration could be reduced to 1·97 s for two particles, this still entailed up to $2\frac{1}{2}$ h CPU time on a CRAY XMP for the particle to travel five diameters. It should be remembered, however, that the current method is not limited to simple geometries and particles of equal density. Further, it is believed that the current computer program can be made more efficient in both the areas of the BEM calculations and the time integration in order to consider multiparticle systems.

ACKNOWLEDGEMENTS

This work was supported by Sandia National Laboratories and the U.S. Department of Energy under contract DE-AC04-76-DP00789.

REFERENCES

1. L. A. Mondy, A. L. Graham and J. L. Jensen, 'Continuum approximations and particle interactions in concentrated suspensions', *J. Rheol.*, **30**, 1031–1051 (1986).
2. A. L. Graham, L. A. Mondy, M. Gottlieb and R. L. Powell, 'Rheological behavior of a suspension of randomly oriented rods', *Appl. Phys. Lett.*, **50**, 127–129 (1987).
3. J. Happel and H. Brenner, *Low Reynolds Number Hydrodynamics*, Martinus Nijhoff Publishers, Dordrecht, 1983.
4. M. E. O'Neill and S. R. Majumdar, 'Asymmetrical slow viscous flow motions caused by the translation or rotation of two spheres. Part II: Asymptotic forms of the solutions when the minimum clearance between the spheres approaches zero.' *Z. Angew. Math. Phys.*, **21**, 180–187 (1970).
5. P. Ganatos, R. Pfeffer and S. Weinbaum, 'A numerical-solution technique for three-dimensional Stokes flows, with applications to the motion of strongly interacting spheres in a plane', *J. Fluid Mech.*, **84**(1), 79–111 (1978).
6. S. Kim and R. T. Mifflin, 'The resistance and mobility functions of two equal spheres in low-Reynolds-number flow', *Phys. Fluids*, **28**, 2033–2045 (1985).
7. S. Kim, 'Sedimentation of two arbitrarily oriented spheroids in a viscous fluid', *Int. J. Multiphase Flow*, **11**(5), 699–712 (1985).
8. L. Durlofsky, J. F. Brady and G. Bossis, 'Dynamic simulation of hydrodynamically interacting particles', *J. Fluid Mech.*, **180**, 21–49 (1987).
9. S. Leichtberg, S. Weinbaum, R. Pfeffer and M. J. Gluckman, 'A study of unsteady forces at low Reynolds number: a strong interaction theory for the coaxial settling of three or more spheres', *Phil. Trans. Roy. Soc. A*, **282**, 585–610 (1976).
10. O. A. Ladyzhenskaya, *The Mathematical Theory of Viscous Incompressible Flow*, Gordon & Breach, New York, 1963.
11. G. K. Youngren and A. Acrivos, 'Stokes flow past a particle of arbitrary shape: a numerical method of solution', *J. Fluid Mech.*, **69**(2), 377–403 (1975).
12. C. A. Brebbia, J. C. F. Telles and L. C. Wrobel, *Boundary Element Techniques*, Springer-Verlag, Berlin, 1984.
13. B. R. Munson and B. K. Gustafson, 'Sensitivity of Stokes flow to geometry', *Exp. Fluids*, **3**, 257–260 (1985).
14. A. K. Mitra and M. S. Ingber, 'The numerical solution of Stokes flow in a domain with re-entrant boundaries by the boundary element method', *Int. j. numer. methods fluids*, **8**, 327–338 (1988).
15. M. Stimson and G. B. Jeffrey, 'The motion of two spheres in a viscous fluid', *Proc. Roy. Soc. A*, **111**, 110–116 (1926).
16. A. J. Goldman, R. G. Cox and H. Brenner, 'The slow motion of two identical arbitrarily oriented spheres through a viscous fluid', *Chem. Eng. Sci.*, **21**, 1151–1170 (1966).